

## Scintillators for high temperature plasma diagnostics

Lukasz Swiderski<sup>1</sup>, Aneta Gojska, Martyna Grodzicka, Stefan Korolczuk, Sławomir Mianowski, Marek Moszynski, Jacek Rzadkiewicz, Paweł Sibczyński, Agnieszka Syntfeld-Kazuch, Marek Szawlowski, Tomasz Szczesniak, Jarosław Szewinski, Adam Szydlowski, Izabella Zychor

National Centre for Nuclear Research (NCBJ)  
05-400 Otwock-Swierk, Poland  
E-mail: lukasz.swiderski@ncbj.gov.pl

Gamma-ray measurements during deuterium-tritium campaigns require detectors characterized by a good energy resolution, a relatively high detection efficiency for a few MeV gamma-rays and a fast response time. Scintillators proposed for monitoring gamma-rays in high temperature plasma experiments fulfill most of these requirements, in addition they are rather resistant to neutron damage in comparison to, e.g., germanium detectors. Intense fast neutron fluxes expected during DT campaigns reduce considered materials to oxygen-free crystals.

CeBr<sub>3</sub> scintillators were investigated with the aim to use them for gamma-ray diagnostics of fusion plasma. Basic properties like light output, energy resolution, decay time and full energy peak detection efficiency were measured using a spectrometry photomultiplier. The response of CeBr<sub>3</sub> was studied as a function of crystal volume between 0.5 and 350 cc. A comparison with well-known and used as reference alkali halide scintillators is presented.

Measurements were performed at the National Centre for Nuclear Research (NCBJ) using gamma-ray sources with energies up to a few MeV, in particular PuBe and PuC gamma emitters. Natural background radiation spectra allowed to estimate the intrinsic activity of CeBr<sub>3</sub> and LaBr<sub>3</sub>:Ce scintillators.

First EPs Conference on Plasma Diagnostics - 1<sup>st</sup> ECPD  
14-17 April 2015,  
Villa Mondragone, Frascati (Rome) Italy

---

<sup>1</sup>Presenting author

## 1. Introduction

One of the methods used in thermonuclear fusion experiments is to trace nuclear fusion products appearing in plasma during discharges. Confined  $\alpha$  particles can undergo reactions with different impurities present in plasma during operation of a fusion device. After the reactions take place, specific gamma rays are emitted [1].

A nuclear reaction  ${}^9\text{Be}(\alpha, n\gamma){}^{12}\text{C}$  between alpha particles and beryllium impurities present in the plasma is used for plasma diagnostics. Gamma ray emitted during this reaction has energy of 4.44 MeV and can be registered outside the fusion device, e.g., JET. Relatively dense materials with high atomic number are required for detection of such a quanta. In addition, detectors should be available in sizes sufficient to absorb the full energy carried out by the gamma-ray. Scintillators are therefore good candidates for gamma spectroscopy in fusion plasma because they are characterized by high stopping power and can be grown in large sizes.

In this work we report on the basic characteristics of different scintillators with possibility to be used in high temperature plasma diagnostics. The tested materials include NaI:Tl, CsI:Tl, LaBr<sub>3</sub>:Ce and CeBr<sub>3</sub> scintillators. The change of detector properties with the size is discussed for CeBr<sub>3</sub> scintillators.

## 2. Experimental details

All tested scintillators were characterized using spectroscopy photomultiplier tubes (PMT) for light readout. The PMTs were chosen accordingly to a size of tested samples, so a cathode photosensitive area was at least of the same size like scintillator output window in order to collect the entire amount of light emitted by the crystal. Beside CsI:Tl, all tested samples were hygroscopic, therefore they were encapsulated by the manufacturers in aluminium housings filled with Teflon reflectors and sealed with quartz windows. CsI:Tl is just slightly hygroscopic, therefore only Teflon tape was used for wrapping the scintillator without hermetically sealed container. Table 1 presents a summary of all samples and used PMTs.

Table 1 List of scintillators and PMTs used in the measurements.

	shape	size (volume)	PMT
CeBr <sub>3</sub>	cuboid	10×10×5 mm <sup>3</sup> (0.5 cc)	R6231
CeBr <sub>3</sub>	cylinder	1"×1" (13 cc)	XP5200
CeBr <sub>3</sub>	cylinder	3"×3" (347 cc)	R6233
LaBr <sub>3</sub> :Ce	cylinder	1"×1" (13 cc)	XP5200
LaBr <sub>3</sub> :Ce	cylinder	3"×3" (347 cc)	XP5700
NaI:Tl	cylinder	1"×1" (13 cc)	XP5200
CsI:Tl	cylinder	1"×1" (13 cc)	XP5200

The signal from the PMT anode fed a charge sensitive preamplifier (either a Canberra 2005 or a Cremat CR-113) and was subsequently passed to a spectroscopy amplifier, e.g., an Ortec 672. The output signal of the amplifier was transferred to a Tukan8k multichannel analyser to record the energy spectra from different  $\gamma$ -ray sources.

The response of tested scintillators to  $\gamma$ -rays was measured in a wide range of energies between 0.1 and 6.1 MeV. The list of used  $\gamma$ -ray sources comprises:  $^{137}\text{Cs}$  (0.662 MeV),  $^{152}\text{Eu}$  ( $\gamma$ -ray lines between 0.122 and 1.408 MeV),  $^{208}\text{Tl}$  (2.615 MeV from natural background radiation),  $^{238}\text{PuBe}$  (4.438 MeV) and  $^{238}\text{PuC}$  (6.129 MeV). Gaussian fits were made for full energy peaks after background subtraction in order to quantify peak centroids, full widths at half maximum (FWHM) and peak areas. The analysis of recorded energy spectra allowed us to evaluate the energy dependence of full energy peak (FEP) detection efficiency and energy resolution for all tested scintillators in the mentioned above  $\gamma$ -ray energy range. The energy resolution was defined as a ratio of the FWHM and the peak centroid.

### 3. Results

#### 3.1. CeBr<sub>3</sub> detection efficiency as a function of scintillator size

The full energy peak (FEP) detection efficiency measured in the energy range between 0.122 MeV and 6.13 MeV for three different size CeBr<sub>3</sub> samples is presented in Fig. 1. The results for 4.44 MeV and 6.13 MeV are not available for the smallest sample as the interaction probability for high energy  $\gamma$ -rays and the intensity of the sources are too low to produce a FEP during acceptable acquisition time (<10<sup>5</sup> s).

The FEP detection efficiency at high energy (above 4 MeV) for the 3"×3" (347 cc) crystal is an order of magnitude larger than for the 1"×1" (13 cc) scintillator. If one extrapolates the results obtained for the 10×10×5 mm<sup>3</sup> (0.5 cc) sample beyond 1.4 MeV, a FEP detection efficiency close to 10<sup>-4</sup> should be expected at a high energy range (above 4 MeV).

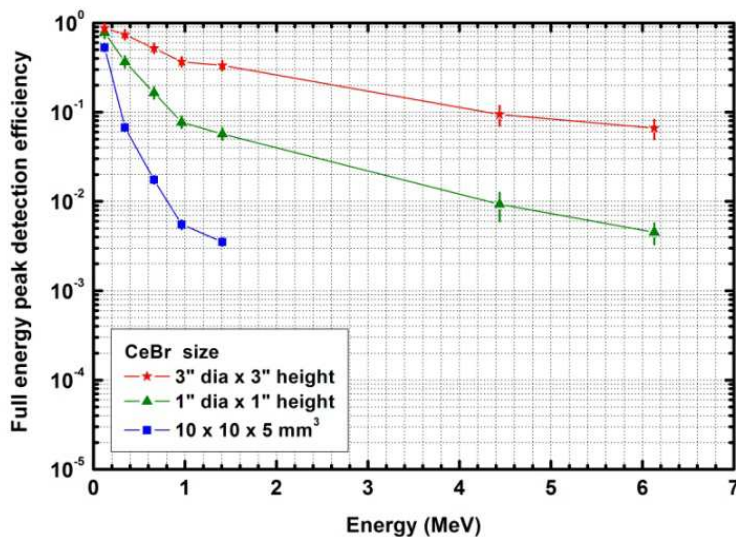


**Fig. 1.**  
Full energy peak (FEP) detection efficiency measured for CeBr<sub>3</sub> crystals.

Fig. 2 presents energy spectra recorded for 1"×1" and 3"×3" CeBr<sub>3</sub> samples irradiated with PuBe source emitting 4.44 MeV  $\gamma$ -rays. Detection of high energy  $\gamma$ -rays in scintillators is mostly connected with positron-electron pair creation. The kinetic energy of created particles is

absorbed in the scintillator and at the end of this process the positron annihilates producing two 511 keV  $\gamma$ -rays. Subsequently, these  $\gamma$ -rays may be absorbed, or they may escape the scintillator with or without Compton scattering inside it. Therefore, besides full energy peak at 4.44 MeV, single escape peak (SEP) is observed at 3.93 MeV if one 511 keV quantum escapes the scintillator without interaction and the second one is absorbed. Double escape peak occurs at 3.42 MeV, when both 511 keV quanta escape without interaction. A Compton continuum is emerging from events when part of 511 keV quanta energy is absorbed. The difference in intensities between FEP, SEP and DEP is caused by different escape probabilities of 511 keV  $\gamma$ -rays produced in small and large samples during absorption of a high energy  $\gamma$ -ray.

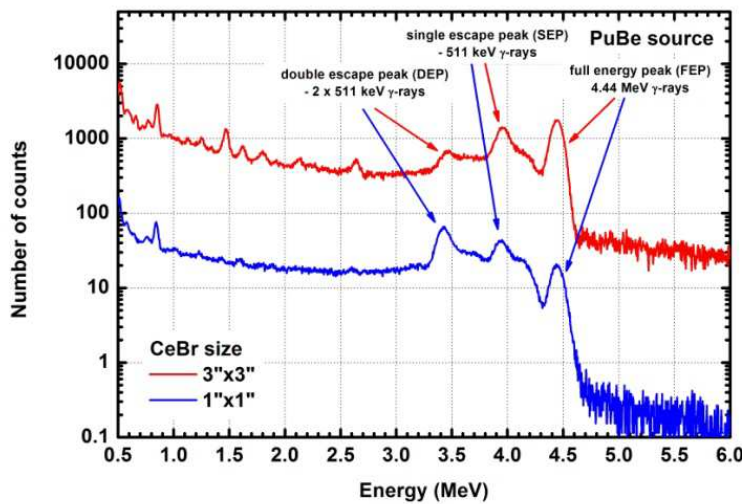


**Fig. 2.**

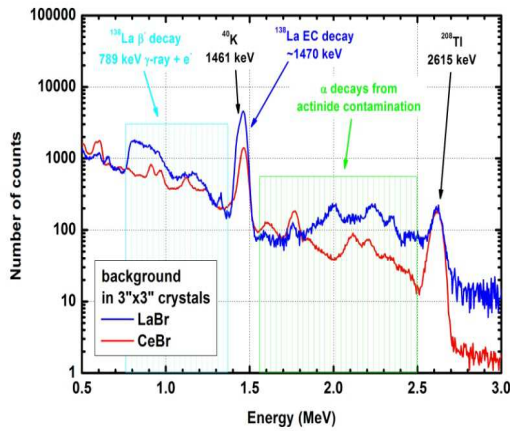
Response of CeBr<sub>3</sub> scintillators to PuBe source emitting 4.44 MeV  $\gamma$ -rays.

Full energy peak, single and double escape peaks are observed.

Spectra were normalized according to acquisition time and  $\gamma$ -ray flux on the detector surface.

### 3.2. Natural background and intrinsic activity in CeBr<sub>3</sub> and LaBr<sub>3</sub>:Ce

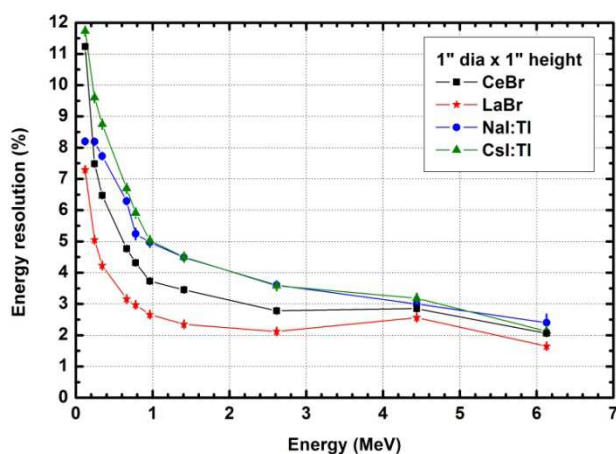
The response of the 3''x3'' CeBr<sub>3</sub> and LaBr<sub>3</sub>:Ce crystals to natural background radiation is presented in Fig. 3. Peaks originating from gamma transitions observed in natural background (1.461 MeV from <sup>40</sup>K and 2.615 MeV from <sup>208</sup>Tl) are clearly seen. Both scintillators show peaks between 1.5 MeV and 2.5 MeV related to contamination by  $\alpha$ -radioactive isotopes from actinides. LaBr<sub>3</sub>:Ce is contaminated also with <sup>138</sup>La decaying by electron capture (EC) or  $\beta^-$ . EC is followed by emission of 1.436 MeV  $\gamma$ -ray and X-ray cascade, giving contribution to a peak at about 1.470 MeV. In addition,  $\beta^-$  decay produces a continuum above 0.789 MeV.

**Fig. 3.**

Response of 3"×3"  $\text{CeBr}_3$  and  $\text{LaBr}_3:\text{Ce}$  to natural background radiation. Events due to internal contamination by actinides are observed between 1.5 MeV and 2.5 MeV.

### 3.3. Comparison of $\text{CeBr}_3$ and $\text{LaBr}_3:\text{Ce}$ with alkali iodide scintillators

The energy resolution of tested scintillator is plotted in Fig. 4 in the energy range between 0.122 and 6.13 MeV.  $\text{LaBr}_3:\text{Ce}$  scintillator shows a superior energy resolution in the entire scanned energy range.  $\text{NaI}:Tl$  and  $\text{CsI}:Tl$  scintillators demonstrate considerably worse energy resolution, even twice in comparison with the  $\text{LaBr}_3:\text{Ce}$ . The  $\text{CeBr}_3$  crystal is characterized by a medium energy resolution. The energy resolution measured at 4.44 MeV does not follow the trend observed for each scintillator due to Doppler broadening effect linked to the emission of 4.44 MeV  $\gamma$ -rays from the excited state of  $^{12}\text{C}$  nuclei, which are the products of the  $^9\text{Be}(\alpha, n\gamma)^{12}\text{C}$  reaction. The lifetime of excited  $^{12}\text{C}$  state is only 61 fs and 4.44 MeV  $\gamma$ -rays are emitted from recoiled nuclei before they are stopped in surrounding materials. This effect is not observed for 6.13 MeV  $\gamma$ -rays from the  $^{13}\text{C}(\alpha, n\gamma)^{16}\text{O}$  reaction because the lifetime of excited state of  $^{16}\text{O}$  is much longer (20 ps) and 6.13 MeV  $\gamma$ -rays are emitted from nuclei at rest [2].

**Fig. 4.**

Energy resolution measured for  $\text{NaI}:Tl$ ,  $\text{CsI}:Tl$ ,  $\text{LaBr}_3:\text{Ce}$  and  $\text{CeBr}_3$  scintillators for  $\gamma$ -ray energies in the range between 0.1 and 6.1 MeV.

Fig. 5 shows the FEP detection efficiency as a function of incident  $\gamma$ -ray energy for 1"×1" scintillators. The CsI:Tl, LaBr<sub>3</sub>:Ce and CeBr<sub>3</sub> crystals have the same FEP detection efficiency in the entire scanned energy range. The NaI:Tl crystal shows substantially lower FEP detection efficiency due to much lower effective atomic number and density compared to other tested crystals.

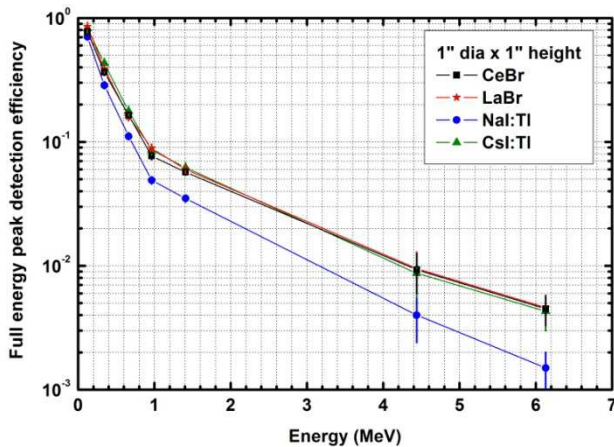


**Fig. 5.**

Full energy peak detection efficiency measured for 1"×1" NaI:Tl, CsI:Tl, LaBr<sub>3</sub>:Ce and CeBr<sub>3</sub> scintillators for  $\gamma$ -ray energies between 0.1 and 6.1 MeV. Lines are plotted to guide the eye.

## 4. Conclusions

High detection efficiency for MeV  $\gamma$ -rays and high stopping power for 511 keV  $\gamma$ -rays, combined with good energy resolution make the LaBr<sub>3</sub>:Ce and CeBr<sub>3</sub> scintillators the most appropriate for plasma diagnostics. CeBr<sub>3</sub> and LaBr<sub>3</sub>:Ce scintillators are well suited for measurements at high counting rates, expected in DT campaigns, because of short scintillation decay times ~15-25 ns.

CeBr<sub>3</sub> has advantages in comparison with LaBr<sub>3</sub>:Ce because of lower internal radioactivity below 1.5 MeV due to lack of any radioactive isotopes.

Full energy peak could be used to detect high energy  $\gamma$ -rays - however, single and double escape peaks may also be used for this purpose.

## Acknowledgements

This scientific work was partly supported by Polish Ministry of Science and Higher Education within the framework of the scientific financial resources in the years 2015-2017 allocated for the realization of the international co-financed project.

## References

- [1] V.G. Kiptily *et al.*, Phys. Rev. Lett. **93** (2004) 115001.
- [2] G. Knoll, *Radiation Detection and Measurement*, 4<sup>th</sup> edition, Wiley 2010.